

Local charge of the $\nu = 5/2$ fractional quantum Hall state

Vivek Venkatachalam¹, Amir Yacoby¹, Loren Pfeiffer² & Ken West²

Electrons moving in two dimensions under the influence of strong magnetic fields effectively lose their kinetic energy and display exotic behaviour dominated by Coulomb forces. When the ratio of electrons to magnetic flux quanta in the system (ν) is near $5/2$, the electrons are predicted to condense into a correlated phase with fractionally charged quasiparticles and a ground-state degeneracy that grows exponentially as these quasiparticles are introduced¹. The only way for electrons to transform between the many ground states would be to braid the fractional excitations around each other. This property has been proposed as the basis of a fault-tolerant quantum computer². Here we present observations of localized quasiparticles at $\nu = 5/2$, confined to puddles by disorder. Using a local electrometer to compare how quasiparticles at $\nu = 5/2$ and $\nu = 7/3$ charge these puddles, we were able to extract the ratio of local charges for these states. Averaged over several disorder configurations and samples, we found the ratio to be $4/3$, suggesting that the local charges are $e_{7/3}^* = e/3$ and $e_{5/2}^* = e/4$, where e is the charge of an electron. This is in agreement with theoretical predictions for a paired state at $\nu = 5/2$. Confirming the existence of localized $e/4$ quasiparticles shows that proposed interferometry experiments to test statistics and computational ability of the state at $\nu = 5/2$ would be possible.

When a two-dimensional electron system (2DES) is subject to a strong perpendicular magnetic field, the physics that emerges is controlled by interelectron Coulomb interactions. If the 2DES is tuned such that ν is near certain rational values, the electrons condense into so-called fractional quantum Hall (FQH) phases³. These strongly correlated states are gapped and incompressible in the bulk of the sample, but metallic and compressible along the sample boundary, allowing current to flow around the perimeter in such a way that the transverse conductance (G_{xy}) is precisely quantized to $G_{xy} = \nu (e^2/h)$, where e is the electron charge and h is Planck's constant. Additionally, the electronic correlations encoded in FQH states give rise to local excitations with a charge a fraction of that of an electron, and braiding statistics that fall outside the conventional classification of bosonic or fermionic. It is predicted that particle interchange can adiabatically evolve a $\nu = 5/2$ system between orthogonal ground states, a property not seen in the state's conventional odd-denominator relatives¹. This property, dubbed non-Abelian braiding statistics, has been proposed as the basis for a topological quantum computer that would be insensitive to environmental decoherence^{2,4}.

One necessary (but insufficient) condition for the existence of exotic braiding statistics at $\nu = 5/2$ is for the ground state to support local excitations with a charge of $e_{5/2}^* = e/4$ (ref. 1). Although a charge of $e/4$ had previously been measured using shot-noise techniques⁵, more-recent data from the same group⁶ suggest that the value of the measured charge changes continuously as the point-contact conductance and temperature are varied, reaching an inferred charge of unity in the weak and strong tunnelling limits. Unexpected charges have also been reported for the more conventional fractions at $1/3$, $2/3$ and $7/3$ (refs 7, 6). Moreover, conductance measurements in the weak tunnelling regime⁸ suggest a quasiparticle charge of $e_{5/2}^* = 0.17e$, in stark contrast to the shot-noise results.

Clearly, a better understanding of the tunnelling processes that take place between quantum Hall edges in the quantum point contact is needed to interpret the shot-noise results. Alternatively, one can infer quasiparticle charge using a thermodynamic approach⁹ that probes the quasiparticle charge in the bulk of the sample. Here we use a single-electron transistor (SET) as a sensitive electrometer to measure the equilibrium charge distribution in the bulk and determine its dependence on the average density and magnetic field. Our results provide clear evidence for quasiparticles at $\nu = 5/2$ with a localized charge of $e/4$.

Our measurement used a fixed SET as a gated device capable of sensitively measuring the local incompressibility ($\kappa^{-1} = \frac{\partial\mu}{\partial n}$, where μ is the local chemical potential and n is the global electron density) of a high-mobility 2DES (ref. 10). The 2DES was in a GaAs/AlGaAs quantum well, grown by molecular beam epitaxy, that was 200 nm deep and 30 nm wide, with symmetric silicon δ -doping layers 100 nm on either side. A metallic back-gate grown 2 μm below the 2DES allowed us to tune n in the well over a typical range of $(2.3\text{--}2.5) \times 10^{15} \text{ m}^{-2}$, with some variation between samples. The SET was fabricated on top of the sample using standard electron-beam lithography and shadow-evaporation techniques (Fig. 1), creating an island

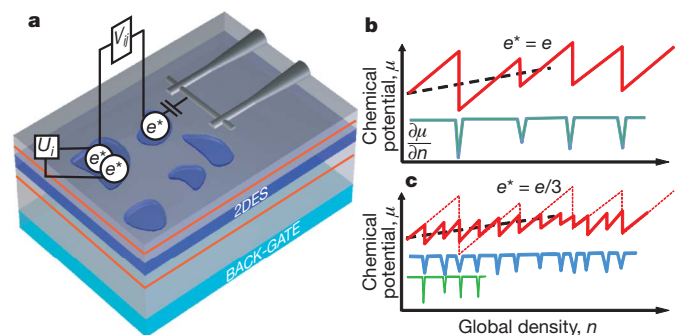


Figure 1 | Filling puddles with fractional charge. **a**, Electrometer used to measure the equilibrium charge distribution in the bulk sample. The quantum well (dark blue, marked 2DES) is 30 nm wide, with symmetric Si δ -doping layers 100 nm on either side (orange bands). Donors in these layers create a disorder potential in the 2DES, which produce puddles of localized states when the bulk is tuned to an incompressible, percolating Hall state. These puddles have some charging energy associated with adding electrons (U_i), and possibly some interaction with surrounding puddles (V_{ij}). Incompressibility ($\kappa^{-1} = \frac{\partial\mu}{\partial n}$) is measured using an SET fabricated on the surface. **b**, Whereas the global chemical potential should increase smoothly with density (black dashed line), the local chemical potential will increase in jumps (red line), with charge being added when the global chemical potential aligns with a localized state. The green line shows the incompressibility of the sample. **c**, Repeating the charging of an identical puddle with objects of charge $e/3$ (solid red line) rather than charge e (dashed red line) results in three times as many charging events in the same range of global density. Scaling the density axis of the charge e spectrum by $1/3$ and shifting it by some amount (green line) should result in good overlap of the incompressibility spectra (blue and green lines).

¹Department of Physics, Harvard University, 11 Oxford Street, Cambridge, Massachusetts 02138, USA. ²Department of Electrical Engineering, Princeton University, Princeton, New Jersey 08544, USA.

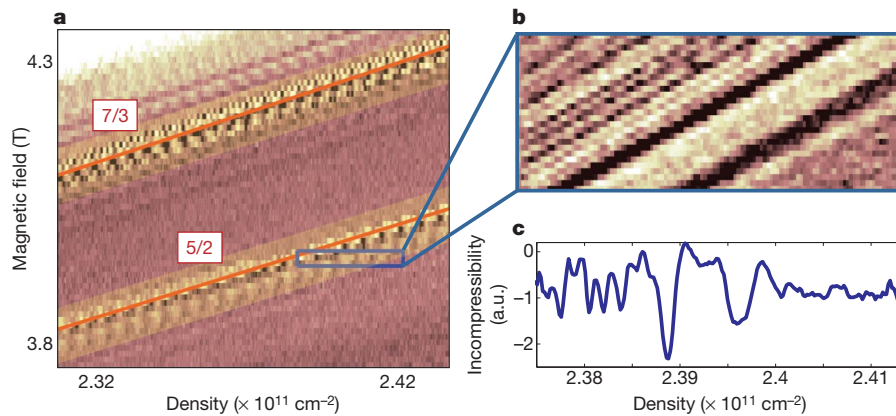


Figure 2 | Incompressibility and localized states at 5/2. **a**, By varying the magnetic field and the back-gate voltage (density), we can identify incompressible phases of the 2DES. Our samples show clear incompressible FQH states at 5/2 and 7/3, with the expected slopes in the nB -plane. **b**, Zooming in shows repeatable

with dimensions $500 \text{ nm} \times 80 \text{ nm}$. All measurements were carried out in a dilution refrigerator with an electron temperature of 20 mK, verified using standard Coulomb blockade techniques.

As we adjust the density and magnetic field (B) we expect to see regions of incompressibility when a gap is present, which will only happen precisely when the system is in a quantum Hall state. The slope of these incompressible regions in the nB -plane corresponds to the filling factor of the state¹¹. Figure 2 shows incompressibility versus density and magnetic field between $\nu = 2$ and $\nu = 3$, with the two highlighted regions corresponding to FQH states at $\nu = 5/2$ and $\nu = 7/3$.

Additionally, owing to the rough disorder potential created by remote donors, we expect different points in space to develop gaps at different values of n . Because of this, we expect a well-developed quantum Hall state to have a percolating incompressible region punctured by small compressible puddles that behave as either dots or antidots¹¹. As n is varied, a given compressible puddle will occasionally be populated by quasiparticles or quasiholes of the surrounding incompressible state. This creates a jump in the local chemical potential, $\mu(n)$, and a spike in the local incompressibility ($\frac{\partial \mu}{\partial n}$). The magnitude and spacing of these spikes is determined by the charging spectrum of the puddle, which in turn is dictated by the quasiparticle charge in the surrounding incompressible region. That is, if the quasiparticle charge were reduced by a factor of three for a fixed disorder potential, we should see three times as many compressible spikes in μ as a function of n (Fig. 1b,c).

This difference in spike frequencies has been used to measure the local charge at $\nu = 1/3$ and $\nu = 2/3$ (ref. 9). Unlike shot-noise measurements⁷, these local compressibility measurements find a quasiparticle charge of $e/3$ at both filling factors. Furthermore, because of the spatial resolution afforded by the scanning technique in that measurement, it was possible to establish that the disorder potential landscape does not change as the electron system is tuned between Hall states with comparable gaps. Transport measurements confirm that the gap inferred from activation of minima in the longitudinal resistance (R_{xx}) is comparable for the states at 5/2 and 7/3 (refs 12, 13), so we can expect similar potential landscapes for the two states.

Our procedure began with obtaining charging spectra (incompressibility versus density) at $\nu = 5/2$ and $\nu = 7/3$. Because the gap for these states is comparable, and the disorder potential is not altered as we change the magnetic field or density, we expect the spacing between charging features to reflect the quasiparticle charge in each state. In the limit of an isolated compressible puddle surrounded by an incompressible fluid, this relationship is particularly simple: if the ratio of local charges between the two spectra is β , the spectra should be identical after one of the density axes is rescaled by a factor of β , and shifted by

charging events associated with quasiparticles localizing in puddles under the SET, stable on a timescale of days. **c**, A linecut showing the charging spectrum of any puddles coupled to the SET. Downwards spikes correspond to quasiparticles entering puddles beneath the SET. a.u., arbitrary units.

some amount (Fig. 3a). To proceed, we chose a value of β and stretched one of the spectra by this factor. We then calculated the correlation $\left(\frac{\langle C_1(x)C_2(x) \rangle}{\sqrt{\langle C_1(x)^2 \rangle \langle C_2(x)^2 \rangle}} \right)$ between the two spectra as a function of density offset and recorded the highest value. We repeated this process for many scaling factors to obtain the best correlation versus β , as depicted in Fig. 3b.

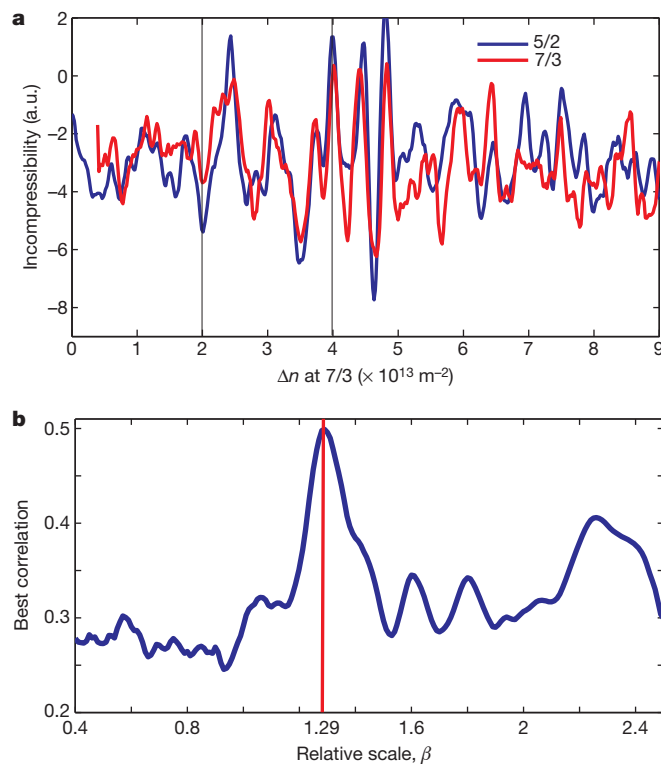


Figure 3 | Comparison of spectra at 5/2 and 7/3. **a**, To determine the charge, we first chose a relative scale between the two density axes (β) and determined the offset between the two spectra that maximized the cross-covariance. Here, the density for the spectrum at 5/2 is scaled up by a factor of 1.29 and shifted to match the spectrum at 7/3. The guide lines show the density change required to add one electron to an area of $100 \text{ nm} \times 500 \text{ nm}$, roughly the size of our SET. We would therefore expect, very roughly, $3 e/3$ charging events in a window this size. Δn , variation in density for the 7/3 (unscaled) trace. **b**, Repeating this for many values of β suggests that a relative scale of 1.29 best describes this data set.

This procedure was repeated for 20 different disorder configurations, obtained by changing samples, measuring with different SETs or thermal cycling to change the disorder. A summary of the data is shown in Fig. 4a, with an average over the measured ensemble in Fig. 4b. Further details regarding the analysis procedure can be found in the Supplementary Material. The peak observed at $\beta = 1.31$ suggests a charge ratio of 4:3 between the two states, and a qualitative inspection of spectra overlap (as in Fig. 3a) corroborates this. To determine the significance of the peak value, we repeated our analysis with pairs of spectra from different disorder configurations, which should be less well correlated. For each scale, we characterized the distribution of best correlations with a mean and standard deviation. These, in turn, can be simply converted to the expected mean and standard error for our data (if it were uncorrelated). The 1σ region around the uncorrelated mean is depicted in red in Fig. 3b. Our averaged correlation at $\beta = 1.31$ lies 3.8 standard errors above the uncorrelated mean, corresponding to a one-tailed P -value of 7×10^{-5} . Assuming a charge of $e_{7/3}^* = e/3$, this measured value of β suggests $e_{5/2}^* = (e/3)/(1.31) = 0.254e$, in agreement with the Moore–Read prediction of $e_{5/2}^* = e/4$ (ref. 1).

To better understand why some configurations seem to provide weaker (and sometimes different) measurements of β , it helps to abandon the assumption that we are charging and monitoring single puddles, as well as the assumption that quasiparticles in different puddles do not interact. A free energy for our system that takes these factors into account is given by:

$$F = \sum_i (\varepsilon_i - V_{BG}) Q_i + \frac{1}{2} \sum_i U_i Q_i (Q_i - 1) + \sum_{i < j} V_{ij} Q_i Q_j - \sum_i \Delta \left[\frac{Q_i}{2} \right]$$

Here, U_i and ε_i are the on-site interaction (self-capacitance) and bare disorder potential for puddle i , respectively. V_{ij} is a pairwise interaction, or cross-capacitance, between puddles i and j , Q_i and Q_j are the charges for puddles i and j respectively, and Δ is the energy gained by forming a bound pair of quasiparticles. V_{BG} is the voltage applied to the backgate and is proportional to the overall number of particles

added. For now, we will let $\Delta = 0$. We assumed that some subset of the puddles is capacitively coupled to and measured by the SET.

To compute charging spectra from this model, we first chose values of U , V and ε for each puddle from Gaussian distributions. We then divided Q_i into discrete units of $e/3$ or $e/4$ and determined how many units of charge to put in each puddle to minimize the above free energy. This was done for each value of V_{BG} , and converted into a charging spectrum. Finally, we took the resulting spectra and repeated the processing performed on the data to obtain summary statistics for comparison. The result, with $\varepsilon = 0 \pm 0.3U$ and $V_{ij} = 0.3U \pm 0.2U$, is shown in Fig. 4c. Results for other parameter choices in a large range are qualitatively similar, with smaller values of σ_ε (uncertainty in ε) and V_{ij} corresponding to sharper peaks and less spread. As expected, these simulations tell us that both ε and V_{ij} can distort spectra in such a way that the maximum cross-covariance will shift slightly or even dramatically away from 4/3. Still, we should always expect some weight at 4/3, and this can be extracted by averaging over disorder configurations (Fig. 4d). There exist two further factors that may contribute to irregular peak spacing in our data that are not considered in the model. First, the 2DES is only truly incompressible for a small range of density, as it transitions into and out of the FQH phase. Outside this range, there is further screening from compressible regions near the puddles of interest that can reduce the effect of the back-gate. Second, there may be quantum effects beyond electrostatics that may alter how quasiparticles in these states charge small puddles.

Recently, there has been some suggestion that $e/2$ quasiparticles may be present at the $\nu = 5/2$ edge and may be relevant to interference measurements¹⁴. In the context of our model, we can consider the effect that weak binding of quasiparticles would have on measured spectra. This binding can be described in terms of the parameter Δ above, and we consider only the case in which pairing affects the $e/4$ quasiparticles. As the strength of pairing is increased relative to the on-site interaction (Fig. 4d), we expect weight to shift from the peak at 4/3 to a peak at 2/3 (corresponding to $e/2$ quasiparticles), with considerable weight at 2/3 even when $\Delta = 0.1U$. Our data show no appreciable evidence for a peak at 2/3, suggesting that the only quasiparticles participating in localization have charge $e/4$. This, however, does not exclude the possibility of $e/2$ excitations on the edge.

To our knowledge, these measurements constitute the first direct measurement of incompressibility and localized states at $\nu = 5/2$, and they provide an equilibrium probe of the local charge that is insensitive to complications arising from measurements of transport through nanostructures. The measured value, $e_{5/2}^* = e/4$, indicates that the FQH state at $\nu = 5/2$ demonstrates pairing, in agreement with proposed non-Abelian variational wavefunctions and differing from other observed FQH states. Finally, the localization of $e/4$ quasiparticles is essential to the development of interferometers capable of detecting and exploiting these exotic braiding properties^{15,16}, and our measurements suggest that $e/4$ localization does indeed occur in a well-behaved way.

Received 14 May; accepted 16 November 2010.

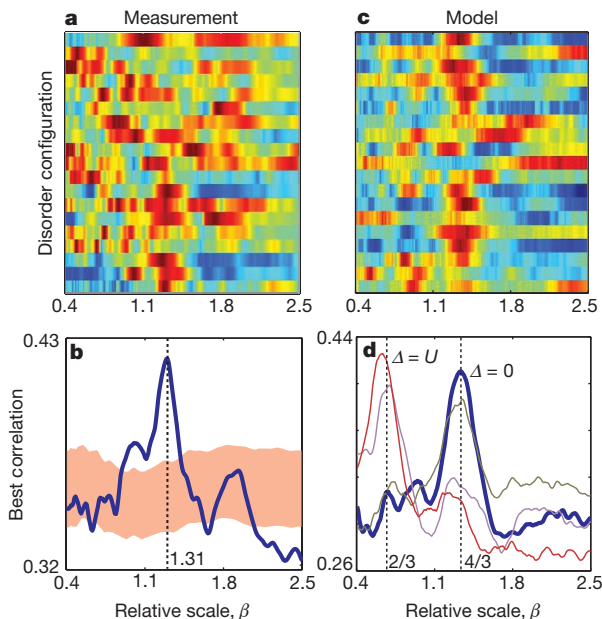


Figure 4 | Summary of data and model. **a**, Repeating the measurement over many disorder configurations and samples shows that the peak at 4/3 is usually present. **b**, Averaging over all measurements yields a clear peak at $\beta = 1.31$, 3.8σ ($P = 7 \times 10^{-5}$) above the uncorrelated background for that scale, colored in orange, suggesting a local charge ratio of 4/3. **c**, **d**, Running our model with parameters $\varepsilon = 0 \pm 0.3$, $V = 0.3 \pm 0.2$ and $\Delta_{5/2} = 0$ (blue), 0.01 (grey), 0.1 (purple) and 1.0 (red) (all in units of U , the on-site charging energy). We simulated charging of four puddles, of which two were capacitively coupled to the SET.

1. Moore, G. & Read, N. Nonabelions in the fractional quantum hall effect. *Nucl. Phys. B* **360**, 362–396 (1991).
2. Nayak, C., Simon, S. H., Stern, A., Freedman, M. & Das Sarma, S. Non-abelian anyons and topological quantum computation. *Rev. Mod. Phys.* **80**, 1083–1159 (2008).
3. Girvin, S. & Prange, R. *The Quantum Hall Effect* (Springer, 1987).
4. Das Sarma, S., Freedman, M. & Nayak, C. Topologically protected qubits from a possible non-abelian fractional quantum hall state. *Phys. Rev. Lett.* **94**, 166802 (2005).
5. Dolev, M., Heiblum, M., Umansky, V., Stern, A. & Mahalu, D. Observation of a quarter of an electron charge at the $\nu = 5/2$ quantum Hall state. *Nature* **452**, 829–834 (2008).
6. Dolev, M. *et al.* Dependence of the tunneling quasiparticle charge determined via shot noise measurements on the tunneling barrier and energetics. *Phys. Rev. B* **81**, 161303 (2010).
7. Bid, A., Ofek, N., Heiblum, M., Umansky, V. & Mahalu, D. Shot noise and charge at the 2/3 composite fractional quantum Hall state. *Phys. Rev. Lett.* **103**, 236802 (2009).
8. Radu, I. *et al.* Quasi-particle properties from tunneling in the $\nu = 5/2$ fractional quantum hall state. *Science* **320**, 899–902 (2008).

9. Martin, J. *et al.* Localization of fractionally charged quasi-particles. *Science* **305**, 980–983 (2004).
10. Ilani, S., Yacoby, A., Mahalu, D. & Shtrikman, H. Microscopic structure of the metal–insulator transition in two dimensions. *Science* **292**, 1354–1357 (2001).
11. Ilani, S. *et al.* The microscopic nature of localization in the quantum hall effect. *Nature* **427**, 328 (2004).
12. Dean, C. R. *et al.* Intrinsic gap of the $\nu = 5/2$ fractional quantum Hall state. *Phys. Rev. Lett.* **100**, 146803 (2008).
13. Choi, H. C., Kang, W., Das Sarma, S., Pfeiffer, L. N. & West, K. W. Activation gaps of fractional quantum hall effect in the second landau level. *Phys. Rev. B* **77**, 081301 (2008).
14. Bishara, W., Bonderson, P., Nayak, C., Shtengel, K. & Slingerland, J. K. Interferometric signature of non-abelian anyons. *Phys. Rev. B* **80**, 155303 (2009).
15. Stern, A. & Halperin, B. I. Proposed experiments to probe the non-abelian $\nu = 5/2$ quantum Hall state. *Phys. Rev. Lett.* **96**, 016802 (2006).
16. Bonderson, P., Kitaev, A. & Shtengel, K. Detecting non-abelian statistics in the $\nu = 5/2$ fractional quantum Hall state. *Phys. Rev. Lett.* **96**, 016803 (2006).

Supplementary Information is linked to the online version of the paper at www.nature.com/nature.

Acknowledgements We would like to acknowledge B. Verdene, J. Waissman and J. Nübler for technical assistance, and B. Halperin for theoretical discussions. We acknowledge financial support from Microsoft Corporation Project Q and the National Science Foundation's Graduate Research Fellowship Program.

Author Contributions V.V. conceived and designed the experiments, prepared samples, carried out the experiments and data analysis, and wrote the paper. A.Y. conceived and designed the experiments, carried out data analysis and wrote the paper. L.P. and K.W. carried out the molecular beam epitaxy growth.

Author Information Reprints and permissions information is available at www.nature.com/reprints. The authors declare no competing financial interests. Readers are welcome to comment on the online version of this article at www.nature.com/nature. Correspondence and requests for materials should be addressed to A.Y. (yacoby@physics.harvard.edu).